

Journal Pre-proofs

Detrital zircons from Late Paleozoic to Triassic sedimentary rocks of the Gongshan-Baoshan Block, SE Tibet: Implications for episodic crustal growth of Eastern Gondwana

Yingtian Song, Li Su, Jinlong Dong, Shuguang Song, Mark B. Allen, Chao Wang, Xiaolan Hu

PII: S1367-9120(19)30458-4
DOI: <https://doi.org/10.1016/j.jseaes.2019.104106>
Reference: JAES 104106

To appear in: *Journal of Asian Earth Sciences*

Received Date: 23 July 2019
Revised Date: 15 October 2019
Accepted Date: 20 October 2019

Please cite this article as: Song, Y., Su, L., Dong, J., Song, S., Allen, M.B., Wang, C., Hu, X., Detrital zircons from Late Paleozoic to Triassic sedimentary rocks of the Gongshan-Baoshan Block, SE Tibet: Implications for episodic crustal growth of Eastern Gondwana, *Journal of Asian Earth Sciences* (2019), doi: <https://doi.org/10.1016/j.jseaes.2019.104106>

This is a PDF file of an article that has undergone enhancements after acceptance, such as the addition of a cover page and metadata, and formatting for readability, but it is not yet the definitive version of record. This version will undergo additional copyediting, typesetting and review before it is published in its final form, but we are providing this version to give early visibility of the article. Please note that, during the production process, errors may be discovered which could affect the content, and all legal disclaimers that apply to the journal pertain.

© 2019 Published by Elsevier Ltd.



Detrital zircons from Late Paleozoic to Triassic sedimentary rocks of the Gongshan-Baoshan Block, SE Tibet: Implications for episodic crustal growth of Eastern Gondwana

Yingtian Song^a, Li Su^{a*}, Jinlong Dong^b, Shuguang Song^b, Mark B. Allen^c, Chao Wang^d

Xiaolan Hu^a

^a *Institute of Earth Sciences, State Key Laboratory of Geological Processes and Mineral Resources, China University of Geosciences, Beijing 100083, China*

^b *MOE Key Laboratory of Orogenic Belts and Crustal Evolution, School of Earth and Space Sciences, Peking University, Beijing 100871, China*

^c *Department of Earth Sciences, Durham University, Durham DH1 3LE, UK*

^d *School of Earth Sciences and Resources, China University of Geosciences, Beijing 100083, China*

Manuscript for *Journal of Asian Earth Sciences*

*Corresponding Author

Li Su

Email: suli@cugb.edu.cn

Abstract

The Gongshan-Baoshan Block is a segment of the northern Sibumasu Terrane, which is a continental strip derived from Eastern Gondwana. However, the formation history of the Gongshan-Baoshan Block and its relationship with other East Gondwana-derived blocks remain unclear. Here, we present five hundred and eighty new analyses of U-Pb ages of detrital zircons from Late Paleozoic to Triassic sedimentary rocks in the Gongshan-Baoshan Block, western Yunnan. The detrital zircon age spectra show distinctive age clusters at 2500-2400 Ma, 1750-1500 Ma, 1200-900 Ma, 600-500 Ma, with a few Archean ages of 3500-2600 Ma, suggesting secular, episodic, continental growth. The age spectra are comparable to those from the Sibumasu Terrane, Australia, Lhasa Block, Qiangtang Block, Tethyan High Himalaya and Cathaysia Block. We confirm that the Gongshan-Baoshan Block and Sibumasu Terrane could have occupied a position outboard of the Lhasa Block and close to northern India, along the northwestern margin of Australia in East Gondwana. The youngest ages from the Mesozoic sediments limit the timing of subduction of the Paleo-Tethys Ocean, which initiated by ~273 Ma and finally stopped at ~223 Ma.

Keywords: Detrital zircon; Gongshan-Baoshan Block; Provenance; East Gondwana; Paleo-Tethys Ocean

1. Introduction

The assembly of Gondwana is considered to have occurred along a network of Pan-African orogenic belts during the Ediacaran to Cambrian (Meert, 2003; Cawood et al., 2007; Bingen et al., 2009). Gondwana has experienced a long-term evolution

affected the course of the global climatic, paleogeographic, geological and biological evolution since its formation (e.g. Veevers, 2004; Poulsen et al., 2008). It is generally divided into East Gondwana and West Gondwana (e.g., Meert and Lieberman, 2008). Most of the terranes which now compose Asia, such as South China, Qiangtang, Sibumasu and Lhasa, originated from East Gondwana (Metcalf, 1996; 2013). Although the outline of major blocks (e.g. India, Australia and East Antarctic) making up the core of East Gondwana is relatively well established, the disposition of small continental fragments on the periphery of East Gondwana is equivocal.

Detrital zircons carry important geological signals due to their stable physical and chemical properties, which can resist the effects of erosion, abrasion, weathering, and even thermal metamorphism. Therefore, detrital zircons from sedimentary rocks have been extensively employed to trace their provenance, constrain maximum depositional ages and to study the reworking and growth of the continental crust (Cawood and Nemchin, 2000; Pullen et al. 2008; Myrow et al., 2010; Zhu et al., 2011; Cai et al., 2017; Zhao et al., 2017).

In this study, we present new zircon U-Pb ages for the Late Paleozoic to Mesozoic strata from the Gongshan-Baoshan Block, west Yunnan. Combined with published detrital zircon ages, paleomagnetic data, Paleozoic strata and fossil assemblages, we provide a new configuration of East Gondwana, and confirm the origin, relationship and position of the continental blocks. We also use these new detrital zircon U-Pb ages to constrain the timing of subduction and closure of the Paleo-Tethys Ocean.

2. Geological background and sample description

The study region is situated in the northern part of the Indochina continent (or Sundaland) (Fig. 1A), a vast triangle-shaped zone bounded by the Sagaing Fault to the west, by the Ailaoshan-Red River Fault to the east and by the Puqu Fault at the northern end (Fig. 1A). It is generally considered to be a region of tectonic escape during the Cenozoic India-Asian continental collision (e.g., Tapponnier et al., 1986; Holt et al., 1991), and it has experienced the long-term and complex tectonic evolution of branches of the Tethyan oceans (Metcalf, 1996, 2013; Jian et al., 2009; Metcalfe et al., 2010; Zhao et al., 2017; Wang et al., 2019a, 2019b). The northern Indochina continent has been intensively modified by deformation since the Cenozoic (e.g., Yin, 2010; Song et al., 2010; van Hinsbergen et al., 2011). According to the subdivision of Metcalfe (2013), tectonic units of the Indochina continent includes, from west to east, the West Burma Block, the Sibumasu Terrane, the Inthanon suture zone, East Malaya Block, Indochina Terrane and South China. The north tip of the continent of our studied region can be further subdivided into the Tengchong Block, Gongshan,-Baoshan Block, Lancangjiang (or Changning-Menglian) suture belt and Lanping-Simao Block (Fig. 1B). The Gongshan and Baoshan regions are not contiguous (Fig. 1) but this separation appears to be the result of Cenozoic shearing, and so the two regions are treated as one block in this paper.

The Tengchong Block is the western portion of the northern Indochina continent and is bordered by the Gaoligong Fault to the east and by the Sagaing Fault to the west (Fig. 1 A and B). The block is regarded as the northern extension of the Mogok

metamorphic belt in Myanmar (Mitchell, 1989; Bertrand et al., 2001). The Tengchong Block is supposed to be a portion of Indian Gondwana in the Late Paleozoic and it could have assembled to Eurasia in the Late Mesozoic (e.g., Morley et al., 2001; Torsvik and Cocks, 2009; Li et al., 2016). It consists principally of low-grade metamorphosed Paleozoic strata, high-grade metamorphic complexes, Mesozoic to Tertiary granitoids and Neogene volcanic-sedimentary sequences (YBGMR, 1990).

The Gongshan Block is an elongated sub-terrane (Fig. 1) and is located between the Gaoligong Fault to the west and the Chongshan Fault to the east. The block mainly comprises Carboniferous-Permian sedimentary strata that have undergone various grades of metamorphism, and unaltered Mesozoic sedimentary strata. High-grade metamorphic complexes (e.g. Gaoligong Group) along the Gaoligong Fault consist of metapelite, leucogranite and migmatitic gneiss and formed in a timing span of 40-20 Ma in response to the southward extrusion of the Indochina continent (Song et al., 2010). Upper Paleozoic strata have experienced low grade metamorphism, but mainly consist of siltstone, sandstone, carbonate rock and shale. Mesozoic sedimentary strata comprise of mudstone, siltstone, sandstone, conglomerate and limestone.

The Baoshan sub-terrane lies to the south, and is bounded by the Gaoligong Fault to the west and by the NS-trending Lancangjiang suture zone to the east (Fig. 1B). The block consists of low-grade metamorphosed, sedimentary strata of Paleozoic age (from Cambrian to Permian), which are unconformably covered by Triassic strata and intruded by Paleozoic to Tertiary granitoids (YBGMR, 1990). The combined Gongshan and Baoshan blocks are considered as the dismembered northern extension of the

Sibumasu Terrane, and have paleontological and stratigraphic affinities to Gondwana (Zhong, 1998; Wang et al., 2001; Fontaine, 2002; Ali et al., 2013; Metcalfe, 2013).

The Lancangjiang suture zone is generally considered to represent the main Paleotethys suture zone in the study area, and it formed via collision between Baoshan Block and Lanping-Simao Block during the Late Permian to Triassic (Jian et al., 2009; Metcalfe, 2011, 2013). The suture zone is connected with the Inthanon suture zone in Thailand (Sone and Metcalfe, 2008), and contains dismembered ophiolitic mélanges, volcanic rocks, deep-water sedimentary rocks and shallow-marine carbonates. High-pressure rocks including lawsonite-bearing eclogite and blueschist with metamorphic ages of ~245-220 Ma have been recently reported (Wang et al., 2019a, 2019b), suggesting a cold oceanic subduction during the northeastern convergence of the Sibumasu Terrane.

The Lanping-Simao Block is bounded by the Changning-Menglian suture zone to the west and separated by the Yangtze Block by the Ailaoshan-Red River fault to the east (Fig. 1 A and B). It comprises the Late Paleozoic volcanic-sedimentary sequences and Triassic sedimentary rocks. The Late Paleozoic volcanic-sedimentary sequences are mainly thick basic to acidic volcanic rocks with terrigenous turbidites formed in a forearc environment (Zhong, 1998). The Triassic sedimentary rocks are distributed along the southwest margin of the block and unconformably overlie pre-Mesozoic strata (YBGMR, 1990; Peng et al., 2006).

Eight samples were collected from the Gongshan-Baoshan Block for zircon U-Pb analysis (see Fig. 1B for localities). They cover the major areas of the elongated block

from north to south and are representative for the provenance of the sedimentation, and thus may constrain the major tectonic events and growth history of the piece of continent. Two of these samples (12NJ66 and 12NJ67) are siltstone from the Triassic Chawalong Formation in the Gongshan region (Fig. 1B). Three samples (12NL68, 12NJ70, and 12NJ71) are low- to medium-grade metamorphic sandstone from the Permian Dingjiazhai Formation in the north part of the Baoshan region (Fig. 1B and C). The other three (17YN01, 17YN14 and 17YN39) are sandstone and collected from the Jurassic Luziqing and Huakaizuo Formations in the south portion of the Baoshan region (Fig. 1B and C). The gray to light gray siltstone is interlayered with limestone and it has millimeter- to centimeter-thick stratification (Fig. 2A). Most siltstones have experienced low-grade metamorphism and been transformed into slate. The sandstone is gray in color and shows centimeter- to meter-thick stratification (Fig. 2B). The siltstone exhibits an oriented aleuritic texture and consists mainly of 65-70 vol.% quartz, 20-25 vol.% sericite, 8-10 vol.% lithics and minor feldspar (Fig. 2C). The siltstone has medium sorting and subangular to sub-rounded roundness, indicating medium to long transportation distances before deposition. The sandstone shows a weak to medium mineral orientation and comprises 95 vol.% quartz, 3-5 vol.% mica and minor feldspar (Fig. 2D). The sandstone is well sorted, indicating long-distance transport before deposition.

3. Analytical methods

The separated detrital zircons from eight sandstone samples were embedded in epoxy resin discs and polished down to about half-sections to expose the grain interiors.

Cathodoluminescence (CL) images were conducted in the School of Earth and Space Sciences, Peking University, by using an FEI QUANTA650 FEG Scanning Electron Microscope (SEM) under conditions of 15 kV/120 nA.

U(-Th)-Pb analyses of the detrital zircons were carried out on an Agilent-7500a quadrupole inductively coupled plasma mass spectrometry coupled with a New Wave SS UP193 laser sampler (LA-ICP-MS) at the Elemental Geochemistry Lab of Institute of Earth Sciences, China University of Geosciences, Beijing (CUGB). Laser spot size is limited as 36 μm with laser energy density of 8.5 J/cm² and a repetition rate of 10 Hz (see Song et al., 2010 for more details). We used zircon 91500 and NIST 610 glass (Wiedenbeck et al., 1995) as external standards, and Si as the internal standard. The zircon TEMORA (417 Ma, Black et al., 2003) and Qinghu (159.5 \pm 0.2 Ma; Li et al., 2013) are used as the secondary standards to supervise the deviation of age measurement/calculation. Data reduction was carried out on the software GLITTER (version 4.4, Macquarie University). The common lead correction was made following Andersen (2002), and Isoplot 3.0 (Ludwig, 2003) was used for age calculations and plots of concordia diagrams.

4. Results

Two samples from Gongshan (12NJ66 and 12NJ67) and six samples from Baoshan (12NJ68, 12NJ70, 12NJ71, 17YN01, 17YN14 and 17YN39) were analysed and the results are listed in Table S1 and Table S2, respectively. Representative CL images are shown in Fig. 3. Diagrams for U-Pb concordia and relative probability density are shown in Figs. 4, 5 and 6. In this study, we only use analytical data that are

less than $\pm 10\%$ discordant. Interpreted ages are based on $^{206}\text{Pb}/^{238}\text{U}$ ages for <1000 Ma grains and on $^{206}\text{Pb}/^{207}\text{Pb}$ ages for >1000 Ma grains (Gehrels, 2000).

4.1 Gongshan Sub-terrane

Detrital zircons from sample 12NJ66 are sub-rounded to subangular in morphology and exhibit equant to long prismatic forms (30-250 μm long) with an aspect ratio of 1:1-4:1 (Fig. 3A). CL images show that most zircon grains are gray to light gray with straight and wide oscillatory growth bands (Fig. 3A). Detrital zircons from sample 12NJ66 have variable Th (18-747 ppm), U (37-1593 ppm) and Th/U ratios (0.03-2.21) (Table S1). Eighty detrital zircons from sample 12NJ66 were analyzed and yielded sixty-nine concordant ages (Fig. 4A). The ages range from 249 ± 4 Ma to 2894 ± 18 Ma (Table S1), with most ages clustered into five major peaks of 912 Ma, 532 Ma, 471 Ma, 363 Ma and 250 Ma, and a few populations of 2889-2398 Ma, 1845-1150 Ma, 900-800 Ma and 721-598 Ma in the relative probability density diagrams (Fig. 4B). Four analyses yield the youngest apparent $^{206}\text{Pb}/^{238}\text{U}$ ages of 270~249 Ma with a mean of 259.2 ± 2.2 Ma (MSWD=0.42; Fig. 4A).

Zircons from sample 12NJ67 are colorless to pale brown, subangular to sub-rounded in morphology and show equant to long prismatic shapes (50-250 μm long) with an aspect ratio of 1.2:1-4:1 (Fig. 3B). CL images show that most zircon grains have clear straight and wide oscillatory growth bands, suggesting magmatic origin (Fig. 3B). Some zircons show core-rim structures and a few zircons lack zoning (Fig. 3B). Detrital zircons from sample 12NJ67 have variable Th (1-912 ppm), U (5-1130 ppm) and Th/U ratios (0.03-2.50) (Table S1). Eighty detrital zircons from sample 12NJ67

were analyzed and yielded seventy-three concordant ages (Fig. 4C). The ages vary from 259 ± 4 Ma to 2668 ± 22 Ma (Table S1), with four major peaks at 1051 Ma, 572 Ma, 511 Ma and 261 Ma, and several subordinate peaks at 2660-2420 Ma, 2125-1129 Ma, 960-793 Ma, and 347 Ma in the relative probability density diagrams (Fig. 4D). Two analyses yield the youngest apparent $^{206}\text{Pb}/^{238}\text{U}$ ages of 259 Ma and 264 Ma (Fig. 4C).

4.2 Baoshan Sub-terrane

Detrital zircons from sample 12NJ68 are colorless to light brown with sub-rounded or round morphology. They have equant to long prismatic forms (30-230 μm long) with length/width ratios of 1:1-3.5:1 (Fig. 3C). CL images indicate that most detrital zircons have core-rim structures and a few ones show gray to light gray internal structures without any zoning (Fig. 3C). Detrital zircons from sample 12NJ68 have varying contents of Th (0.1-9127 ppm) and U (12-1023 ppm) with a wide range of Th/U ratios (0.01-4.20) (Table S2). Eighty detrital zircons from sample 12NJ68 were analyzed and yielded seventy-three concordant ages (Fig. 5A). The ages vary from 377 ± 6 Ma to 3526 ± 13 Ma (Table S2), with four major peaks at 1142 Ma, 950 Ma, 848 Ma and 568 Ma, and several subordinate peaks at 3524-2704 Ma, 2410-2306 Ma, 1964-1558 Ma, and 382-376 Ma in the relative probability density diagrams (Fig. 5B).

Detrital zircons from sample 12NJ70 are colorless to light brown and transparent with subangular to angular morphology. They have equant to long prismatic forms (20-200 μm long) with length/width values of 1.2:1-4:1 (Fig. 3D). CL images indicate that most detrital zircons display features of zircon grains of magmatic origin with wide and straight oscillatory growth bands (Fig. 3D). Detrital zircons from sample 12NJ70 have

varying concentrations of Th (43-1653 ppm) and U (98-3230 ppm) with Th/U ratios of 0.03-1.85 (Table S2). Seventy-five detrital zircons from sample 12NJ70 were analyzed and yielded sixty-one concordant ages (Fig. 5C). The ages vary from 330 ± 5 Ma to 2452 ± 18 Ma (Table S2), with two major peaks at 902 Ma and 492 Ma, and several subordinate peaks at 2428 Ma, 1751-1405 Ma, 1063 Ma, 825-754 Ma, 689 Ma, 455-408 Ma and 328 Ma in the relative probability density diagrams (Fig. 5D).

Detrital zircons from sample 12NJ71 are transparent and colorless to pale brown with sub-rounded to angular morphology. They have equant to long prismatic forms (50-250 μm long) with length/width ratios of 1.2:1-3.5:1 (Fig. 3E). CL images show that most detrital zircons have straight and wide oscillatory growth bands and a few grains possess core-rim structures (Fig. 3E). Detrital zircons from sample 12NJ71 have varying contents of Th (7-1004 ppm) and U (68-3852 ppm) with Th/U values of 0.04-2.40 (Table S2). Eighty detrital zircons from sample 12NJ71 were analyzed and yielded seventy-one concordant ages (Fig. 5E). The ages vary from 507 ± 8 Ma to 3427 ± 24 Ma (Table S2), with six major peaks at 2441 Ma, 955 Ma, 861 Ma, 770 Ma, 577 Ma and 540 Ma, and several subordinate peaks at 3403-2576 Ma, 2053 Ma, 1715 Ma, 1422 Ma, 1164 Ma and 1072 Ma in the relative probability density diagrams (Fig. 5F). One analysis gives the youngest apparent $^{206}\text{Pb}/^{238}\text{U}$ ages of 507 ± 8 Ma (Fig. 5E; Table S2).

Detrital zircons from sample 17YN01 are transparent and colorless to pale brown with sub-rounded to angular morphology. They have equant to long prismatic forms (50-300 μm long) with an aspect ratio of 1.2:1-4:1 (Fig. 3F). CL images show that most detrital zircons have weak oscillatory growth bands and a few grains possess gray to

light gray internal structures without any zoning (Fig. 3F). Detrital zircons from sample 17YN01 have varying contents of Th (13-419 ppm) and U (28-992 ppm) with Th/U values of 0.03-2.50 (Table S2). Eighty detrital zircons from sample 17YN01 were analyzed and yielded seventy-eight concordant ages (Fig. 6A). The ages vary from 526 ± 8 Ma to 3436 ± 24 Ma (Table S2), with two major peaks at 910 Ma and 564 Ma, and several subordinate peaks at 3420-2398 Ma, 1696 Ma, 1426 Ma and 1054 Ma in the relative probability density diagrams (Fig. 6B). Fifteen analyses yield the youngest apparent $^{206}\text{Pb}/^{238}\text{U}$ ages of 584~526 Ma with a mean of 562.2 ± 8.1 Ma (MSWD=4.2; Fig. 6A).

Detrital zircons from sample 17YN14 are colorless to light brown and transparent with subangular to angular morphology. They have equant to long prismatic forms (20-320 μm long) with length/width ratios of 1.2:1-3.2:1 (Fig. 3G). CL images display that detrital zircons have features of zircon grains of magmatic origin, with clear wide and straight oscillatory growth bands (Fig. 3G). Detrital zircons from sample 17YN14 have varying contents of Th (4-1939 ppm) and U (14-856 ppm) with Th/U values of 0.02-2.38 (Table S2). Eighty detrital zircons from sample 17YN14 were analyzed and yielded seventy-six concordant ages (Fig. 6C). The ages vary from 223 ± 3 Ma to 3292 ± 17 Ma (Table S2), with four major peaks at 1123 Ma, 593 Ma, 499 Ma and 225 Ma, and several subordinate peaks at 3279-2383 Ma, 1895-1461 Ma, 929 Ma, 735-652 Ma in the relative probability density diagrams (Fig. 6D). Five analyses yield the youngest apparent $^{206}\text{Pb}/^{238}\text{U}$ ages of 245~223 Ma with a mean of 232 ± 12 Ma (MSWD=8.7; Fig. 6C).

Detrital zircons from sample 17YN39 are colorless to light brown and transparent with round to subangular morphology. They have equant to long prismatic forms (40-250 μm long) with length/width ratios of 1:1-3.5:1 (Fig. 3H). CL images display that detrital zircons have features of zircon grains of magmatic origin, with clear wide and straight oscillatory growth bands (Fig. 3H). Detrital zircons from sample 17YN39 have varying contents of Th (11-489 ppm) and U (16-1176 ppm) with Th/U values of 0.08-2.22 (Table S2). Eighty detrital zircons from sample 17YN39 were analyzed and yielded seventy-nine concordant ages (Fig. 6E). The ages vary from 263 ± 3 Ma to 3255 ± 35 Ma (Table S2), with four major peaks at 956 Ma, 478 Ma, 409 Ma and 266 Ma, and several subordinate peaks at 3232 Ma, 2786 Ma, 2473 Ma, 1855-1473 Ma, 1022 Ma, 864-591 Ma and 369 Ma in the relative probability density diagrams (Fig. 6F). Four analyses yield the youngest apparent $^{206}\text{Pb}/^{238}\text{U}$ ages ranging from 263 to 273 Ma with a mean of 266.8 ± 6.5 Ma (MSWD=1.3; Fig. 6E).

5. Discussion

5.1 Provenance analysis

In order to distinguish the provenance of the Late Paleozoic to Triassic sedimentary rocks from Gongshan-Baoshan Block, we compiled U-Pb geochronological detrital zircon data published from the north segment of the Sibumasu terrane, Western Australia, Eastern Australia, Lhasa Block, western Qiangtang, Tethyan Himalaya, High Himalaya and Cathaysia Block (Fig. 7).

In this study, the sedimentary samples from the Gongshan-Baoshan Block are quartz-rich and lithic-poor (Fig. 2B and C) and detrital zircon grains are round to

subangular (Fig. 3), indicating that these zircons underwent long-distance transport before sedimentation. Additionally, the oldest granitic plutons in Gongshan-Baoshan Block were dated at 502-459 Ma (Song et al., 2007; Liu et al., 2009; Li et al., 2012), and the exposed Precambrian basement has not been determined so far. These data imply that detrital zircons from the Gongshan-Baoshan Block could have originated from broad sources over a large region of a continent.

The major peaks of detrital zircon age spectra from Gongshan are at 1135 Ma, 1051 Ma, 914 Ma, 573 Ma and 263 Ma with subordinate peaks at 2415 Ma, 1843-1378 Ma, 472 Ma and 358 Ma (Fig. 7A), and from Baoshan, have similar major peaks of 1072 Ma, 948 Ma, 570 Ma, 496 Ma and 266 Ma with subordinate peaks at 2418 Ma, 1702 Ma, 1436 Ma and 368 Ma (Fig. 7B).

Detrital zircon age populations of Paleozoic strata from the northern Sibumasu Terrane have major peaks centered at 1162 Ma, 1070 Ma, 990 Ma and 506 Ma with subordinate populations of 2422 Ma and 1712 Ma (Fig. 7C) (Cai et al., 2017). Detrital zircon age populations in Western Australia are clustered into dominant peaks at 1197 Ma and 518 Ma with subordinate peaks at 2617 Ma, 1638 Ma and 274 Ma (Fig. 7D) (Cawood and Nemchin, 2000; Veevers et al., 2005). On the other hand, detrital zircon age populations of the Late Carboniferous to Triassic strata from Eastern Australia are characterized by major peaks centered at 1197 Ma, 1086 Ma, 571 Ma, 500 Ma and 465 Ma with subordinate peaks at 2715 Ma, 2485 Ma, 2209 Ma, 941 Ma and 359 Ma (Fig. 7E) (Phillips et al., 2018). The unique peak at 1197 Ma shown in Fig. 7D and E is possibly derived from the Albany-Fraser orogenic belt in southwestern Australia with

magmatism at 1330-1130 Ma (Clark et al., 2000; Fitzsimons, 2000a). Detrital zircon age populations of the Carboniferous to Cretaceous strata from the Lhasa Block show major peaks at 1148 Ma and 542 Ma with subordinate peaks at 1852 Ma, 1574 Ma and 938 Ma (Fig. 7F) (Leier et al., 2007; Zhu et al., 2011), resembling those from Australia (Fig. 7D and E).

Detrital zircon age spectra of the Paleozoic strata from western Qiangtang are mainly clustered at 962 Ma and 530 Ma with secondary peaks at 2466 Ma and 624 Ma (Fig. 7G) (Pullen et al., 2008; Zhu et al., 2011; Dong et al., 2011). Detrital zircon age spectra of the Paleozoic strata from Tethyan Himalaya are mainly clustered into 957 Ma with secondary peaks at 2464 Ma, 1720 Ma, 614 Ma and 528 Ma (Fig. 7H) (McQuarrie et al., 2008; Myrow et al., 2009, 2010; Zhu et al., 2011). Detrital zircon age populations of the Paleozoic strata from High Himalaya are mainly clustered into 1172 Ma, 983 Ma and 962 Ma with subordinate peaks at 2574 Ma, 1593 Ma and 497 Ma (Fig. 7I) (Gehrels et al., 2006a, 2006b). Detrital zircon age spectra of the Paleozoic strata from Cathaysia Block are mainly clustered into 2454 Ma, 1113 Ma and 531 Ma with secondary peaks at 2796 Ma, 2000-1545 Ma, 1239 Ma, 767 Ma and 645 Ma (Fig. 7J) (Yao et al., 2011). The unique peaks at 983-957 Ma in western High Himalaya, Tethyan Himalaya, Qiangtang and Cathaysia Block are considered to be originated from the Rayner/Ghats Province in India and Antarctica with detrital zircon ages of 990-900 Ma (Boger et al., 2000; Cawood et al., 2013).

The aggregation of East Gondwana produced the Prydz-Darling orogenic belt (600-500 Ma) between southwest Australia, India and Antarctic (Fig. 8) (e.g., Cawood

et al., 2007; Meert and Lieberman, 2008). The Prydz-Darling orogenic belt is considered to provide a significant sediment source for the Sibumasu Terrane, Australia, Lhasa, western Tethyan Himalaya, High Himalaya, Qiangtang and the Cathaysia Block (Fig. 8) (e.g., Cawood et al., 2013; Cai et al., 2017; Zhang et al., 2018). Given the dominant peaks at 600-500 Ma, the Prydz-Darling orogenic belt was also likely to be an important sediment source for the Gongshan-Baoshan Block (Fig. 7A and B). Likewise, the Rayner/Ghats Province (990-900 Ma) in India and Antarctica and the Albany-Fraser orogenic belt (1330-1130 Ma) in southwestern Australia are also important sources for the Permian to Jurassic strata from the Gongshan-Baoshan Block (Fig. 8). In addition, a specific peak at 1072-1050 Ma occurs in our samples (Fig. 7A and B), and it could be derived from the Maud Province in southern East Antarctica, which contains zircons with ages of 1090-1030 Ma (Fig. 8) (Fitzsimons, 2000b).

It is notable that the Gongshan-Baoshan Block has an age population of 420-330 Ma, similar to Eastern Australia and Lhasa Block (Fig 7), suggesting a Variscan-aged magmatic event. The youngest age population of 273-223 Ma in our samples (Fig. 7A and B) could be sourced from the arc related to the Lanchangjiang suture zone.

5.2 Paleogeographic relationships between the Gongshan-Baoshan Block and other East Gondwana-derived terranes

As shown in Fig. 7A and B, the presence of 1330-900 Ma (Grenville age) and 600-500 Ma (Pan-African age) detrital zircons in this study are typical features of a Gondwana-derived source (e.g., Myrow et al., 2010; Metcalfe, 2013; Cawood et al., 2013; Zhang et al., 2018). The Gongshan-Baoshan Block has the detrital zircon

hallmarks related to the assembly of Gondwana.

Detrital zircon age spectra from the Gongshan-Baoshan Block are very similar to those from Sibumasu Terrane (Fig. 7A-C), indicating that the two blocks could have been united and have experienced the same tectonic evolution. The presence of 1330-1130 Ma detrital zircons in the blocks indicates that they could have originated from Australia. The inference is supported by similar Paleozoic strata, fossil assemblages and palaeoenvironment proxies (Fang et al., 2000; Agematsu and Sashida, 2009; Metcalfe, 2013; Li et al., 2015). It is generally considered that the Lhasa Block could be situated at the northwestern margin of Australia (e.g., Zhu et al., 2011; Metcalfe, 2013; Zhang et al., 2018). Notably, the detrital zircon age proportion at 1330-1130 Ma from the Lhasa Block is 19.9%, which is far more than the Gongshan-Baoshan Block and Sibumasu Terrane (12.7%, 8.9% and 10.2%, respectively), indicating that the two blocks could have occupied a position outboard of the Lhasa Block, along the northwestern margin of Australia. In contrast, the detrital zircon age proportion at 990-900 Ma from the Lhasa Block (6.6%) is much less than those from Gongshan-Baoshan Block and northern Sibumasu Terrane (12.0%, 13.0% and 17.9%, respectively). In addition, some paleomagnetic studies have documented that Baoshan was located close to the junction of northwestern Australia and northern India during the Paleozoic time (Ali et al., 2013; Xu et al., 2015). The lines of evidence indicate that the Gongshan-Baoshan Block and northern Sibumasu Terrane could be closer to northern India than the Lhasa Block.

Taking detrital zircon age patterns, paleomagnetic data, Paleozoic strata and fossil

assemblages into consideration, we propose that the Gongshan-Baoshan Block and Sibumasu Terrane are a uniform continental segment and could occupy a position outboard the Lhasa Block close to northern India along the northwestern margin of Australia in East Gondwana (Fig. 8).

5.3 Episodic growth of the Eastern Gondwana continent

The detrital zircons from the Gongshan-Baoshan Block, northern Sibumasu Terrane, Western Australia, Eastern Australia, Lhasa Block, western Qiangtang, Tethyan Himalaya, High Himalaya and Cathaysia Block are in six major periods, which are: 3500-3000 Ma, 2800-2600 Ma, 2500-2400 Ma, 1800-1500 Ma, 1400-900 Ma and 600-500 Ma (Fig. 7). These major age intervals reveal that the East Gondwana continent has undergone episodic growth.

The 3500-3000 Ma age group was related to the formation of continental nuclei. Archean continental growth occurred at 2800-2600 Ma. Except for Western Australia and High Himalaya, a unique peak at 2500-2400 Ma from other terranes indicates that orogenesis or cratonization in the end of Archean could have extended to the Paleoproterozoic on the Earth. The age of 1800-1500 Ma was associated with assembly of the Columbia supercontinent, which was considered to be the timing of final assembly of Columbia (or Nuna) Supercontinent (Pourteau et al., 2018). The age of 1400-900 Ma resulted from the Grenvillian orogeny (assembly of Rodinia), and the age of 600-500 Ma was connected with assembly of Gondwana.

5.4 Timing of subduction initiation and closure of the Paleo-Tethys Ocean

It is generally thought that the Paleo-Tethys Ocean had experienced a long period of history since the Late Cambrian (e.g. Zhai et al., 2013, 2016). The initiation of subduction and final closure of the Paleo-Tethys Ocean, however, is poorly constrained.

In the Gongshan-Baoshan Block, the Paleozoic strata (Cambrian to Permian) show characteristics of stable sedimentary deposits from a shallow marine environment. The Triassic strata, on the other hand, unconformably overlie on the Paleozoic strata (Cambrian to Permian), suggesting a different sedimentary setting, likely a back-arc basin behind the Lancangjiang arc in the east.

The ages of arc igneous rocks along the Lancangjiang suture zone range from 213 Ma to 255 Ma (Wang et al., 2014; Chen et al., 2016). Based on ages of the SSZ ophiolite (270-264 Ma), Jian et al. (2009) suggested the subduction of the main Paleo-Tethys Ocean started in the Permian. High-pressure (HP) metamorphic terranes along the Central Qiangtang-Lancangjiang suture zone have uniform ages of 245-220 Ma (Zhai et al., 2011; Wang et al., 2019a, 2019b), indicating that the Paleo-Tethys Ocean closed at or before 220 Ma.

In this study, the sixteen youngest detrital zircon ages range from 223 to 273 Ma (Tables S1 and S2). The youngest detrital zircons are euhedral to subhedral with CL images showing magmatic origin (Fig. 3). The 223 Ma age is consistent with ones of the HP metamorphic terranes along the Central Qiangtang-Lancangjiang suture (Zhai et al., 2011; Wang et al., 2019a, 2019b), and the 273 Ma age is nearly synchronous with

the SSZ ophiolite in Lancangjiang suture zone (270-264 Ma; Jian et al., 2009). Our new detrital zircon ages indicate that subduction of the Paleo-Tethys Ocean most likely initiated at ~273 Ma and ended at ~223 Ma.

6. Conclusions

(1) The detrital zircons of the Permian to Jurassic strata from the Gongshan-Baoshan Block reveal that secular episodic continental growth focused on the time periods 2500-2400 Ma, 1750-1500 Ma, 1200-900 Ma, 600-500 Ma, with a few Archean ages of 3500-2600 Ma.

(2) The detrital zircon age patterns show that the Gongshan-Baoshan Block is part of the larger Sibumasu Terrane, and could have been located outboard of the Lhasa Block, close to northern India, along the northwestern margin of Australia in Eastern Gondwana.

(3) Our results constrain that the timing of subduction of the Paleo-Tethys Ocean initiated at ~273 Ma and ended at ~223 Ma.

Acknowledgements

This work was financially supported by the National Natural Science Foundation of China (grants 41572040, 41372060). We thank the editor and reviewers for their time and efforts to this manuscript.

References

Andersen, T., 2002. Correction of common lead in U-Pb analyses that do not report ^{204}Pb . *Chem. Geol.* 192, 59–79.

Ali, J.R., Cheung, H.M.C., Aitchison, J.C., Sun, Y., 2013. Palaeomagnetic re-

investigation of Early Permian rift basalts from the Baoshan block, SW China: constraints on the site-of-origin of the Gondwana-derived eastern Cimmerian terranes. *Geophys. J. Int.* 193:650–663.

Agematsu, S., Sashida, K., 2009. Ordovician sea-level change and paleogeography of the Sibumasu terrane based on the conodont biostratigraphy. *Paleontol. Res.* 13, 327–336.

Black, L.P., Kamo, S.L., Allen, C.M., Aleinikoff, J.N., Davis, D.W., Korsch, R.J., Foudoulis, C., 2003. TEMORA 1: a new zircon standard for Phanerozoic U–Pb geochronology. *Chem. Geol.* 200, 155–170.

Boger, S.D., Carson, C.J., Wilson, C.J.L., Fanning, C.M., 2000. Neoproterozoic deformation in the Radok Lake region of the northern Prince Charles Mountains, east Antarctica; evidence for a single protracted orogenic event. *Precambrian Res.* 104, 1–24.

Bingen, B., Jacobs, J., Viola, G., Henderson, I.H.C., Skår, Ø., Boyd, R., Thomas, R.J., Solli, A., 2009. Geochronology of the Precambrian crust in the Mozambique belt in NE Mozambique, and implications for Gondwana assembly. *Precamb. Res.* 170, 231–255.

Bian, W., Yang, T., Ma, Y., Jin, J., Gao, F., Wang, S., Prng, W., Zhang, S., Wu, H., Li, H., Cao, L., Shi, Y., 2019. Paleomagnetic and geochronological results from the Zhela and Weimei Formations lava flows of the eastern Tethyan Himalaya: New insights into the breakup of eastern Gondwana. *J. Geophys. Res.* 124, 44–64.

Cai, F.L., Ding, L., Yao, W., Laskowski, A.K., Xu, Q., Zhang, J.E., Sein, F., 2017.

- Provenance and tectonic evolution of Lower Paleozoic–Upper Mesozoic strata from Sibumasu Terrane, Myanmar. *Gondwana Res.* 41, 325–336.
- Cawood, P.A., Nemchin, A.A., 2000. Provenance record of a rift basin: U/Pb ages of detrital zircons from the Perth Basin, Western Australia. *Sediment. Geol.* 134, 209–234.
- Cawood, P.A., Johnson, M.R.W., Nemchin, A.A., 2007. Early Palaeozoic orogenesis along the Indian margin of Gondwana: tectonic response to Gondwana assembly. *Earth Planet. Sci. Lett.* 255, 70–84.
- Cawood, P.A., Wang, Y., Xu, Y., Zhao, G., 2013. Locating South China in Rodinia and Gondwana: a fragment of greater India lithosphere? *Geology* 41:903–906.
- Clark, D.J., Hensen, B.J., Kinny, P.D., 2000. Geochronological constraints for a two stage history of the Albany-Fraser Orogen, Western Australia. *Precamb. Res.* 102, 155–183.
- Chen, S.-S., Shi, R.-D., Yi, G.-D., Zou, H.-B., 2016. Middle Triassic volcanic rocks in the Northern Qiangtang (Central Tibet): Geochronology, petrogenesis, and tectonic implications. *Tectonophysics* 666, 90-102.
- Dong, C., Li, C., Wan, Y., Wang, W., Wu, Y., Xie, H., Liu, D., 2011. Detrital zircon age model of Ordovician Wenquan quartzite south of Lungmuco-Shuanghu suture in the Qiangtang area, Tibet: constraint on tectonic affinity and source regions. *Sci. China Earth Sci.* 54, 1034–1042.
- Fontaine, H., 2002. Permian of Southeast Asia: an overview. *J. Asian Earth Sci.* 20, 567–588.

- Fitzsimons, I. C.W., 2000a. Grenville-age basement provinces in East Antarctica: evidence for three separate collisional orogens. *Geology* 28, 879–882.
- Fitzsimons, I.C.W., 2000b. A review of tectonic events in the East Antarctic shield, and their implications for Gondwana and earlier supercontinents. *J. Afr. Earth Sci.* 31, 3 – 23.
- Fang, Z.J., Wang, Y.J., Shi, G.R., Zhou, Z.C., Xiao, Y.W., 2000. On the age of the Dingjiazhai Formation of Baoshan Block, western Yunnan, China-with a discussion on the redeposition hypothesis. *Acta Palaeontol. Sinica* 39 (2), 267–278 (in Chinese with English abstract).
- Gehrels, G.E., 2000. Introduction to detrital zircon studies of Paleozoic and Triassic strata in western Nevada and northern California. In: Soreghan, M.J., Gehrels, G.E. (Eds.), *Paleozoic and Triassic Paleogeography and Tectonic Evolution of Western Nevada and Northern California*. *Geol. Soc. Am. Spec. Pap.*, pp. 1–17.
- Gehrels, G.E., DeCelles, P.G., Ojha, T.P., Upreti, B.N., 2006a. Geological and U-Pb geochronologic evidence for early Paleozoic tectonism in the Dadeldhura thrust sheet, far-west Nepal Himalaya. *J. Asian Earth Sci.* 28, 385–408.
- Gehrels, G.E., DeCelles, P.G., Ojha, T.P., and Upreti, B.N., 2006b. Geologic and U-Th-Pb geochronologic evidence for early Paleozoic tectonism in the Kathmandu thrust sheet, central Nepal Himalaya. *Geol. Soc. Am. Bull.* 118, 185–198.
- Holt, W.E., Ni, J.F., Wallace, T.C., Haines, A.J., 1991. The active tectonics of the eastern Himalayan syntaxis and surrounding regions. *J. Geophys. Res. Solid Earth Planets* 96 (B9), 14595–14632.

- Huang, H., Shi, Y.K., Jin, X.C., 2015. Permian fusulinid biostratigraphy of the Baoshan Block in western Yunnan, China with constraints on paleogeography and paleoclimate. *J. Asian Earth Sci.* 104, 127–144.
- Jian, P., Liu, D.Y., Kröner, A., Zhang, Q., Wang, Y.Z., Sun, X.M., Zhang, W., 2009. Devonian to Permian plate tectonic cycle of the Paleo-Tethys Orogen in southwest China (I): geochemistry of ophiolites, arc/back-arc assemblages and within-plate igneous rocks. *Lithos* 113, 748–766.
- Li, D., Chen, Y., Hou, K., Luo, Z., 2016. Origin and evolution of the Tengchong block, southeastern margin of the Tibetan Plateau: Zircon U-Pb and Lu-Hf isotopic evidence from the (meta-) sedimentary rocks and intrusions. *Tectonophysics* 687, 245–256.
- Ludwig, K.R., 2003. ISOPLOT 3.0: a geochronological toolkit for Microsoft Excel. *Berkeley Geochronol. Center Special Publ.* 4, 25–31.
- Liao, S.Y., Wang, D.B., Tang, Y., Yin, F.G., Cao, S.N., Wang, L.Q., Wang, B.D., Sun, Z.M., 2015. Late Paleozoic Woniusi basaltic province from Sibumasu terrane: implications for the breakup of eastern Gondwana's northern margin. *Geol. Soc. Am. Bull.* 127, 1313–1330.
- Leier, A.L., Paul, K., Gehrels, G.E., Decelles, P.G., 2007. Detrital zircon geochronology of carboniferous–cretaceous strata in the Lhasa terrane, southern tibet. *Basin Res.* 19, 361–378.
- Liu, S., Hu, R.Z., Gao, S., Feng, C.X., Huang, Z.L., Lai, S.C., Yuan, H.L., Liu, X.M., Coulson, I.M., Feng, G.Y., Wang, T., Qi, Y.Q., 2009. U-Pb zircon, geochemical

- and Sr–Nd–Hf isotopic constraints on the age and origin of Early Palaeozoic I-type granite from the Tengchong-Baoshan Block, Western Yunnan Province, SW China. *J. Asian Earth Sci.* 36, 168–182.
- Li, Z.H., Lin, S. L., Cong, F., Xie, T., Zou, G. F., 2012. U-Pb ages of zircon from metamorphic rocks of the Gaoligongshan Group in western Yunnan and its tectonic significance. *Acta Petrol. Sin.* 28(5), 1529–1541 (in Chinese with English abstract).
- Li, G.J., Wang, Q.F., Huang, Y.H., Chen, F.C., Dong, P., 2015. Discovery of Hadean–Mesoarchean crustal materials in the northern Sibumasu block and its significance for Gondwana reconstruction. *Precambrian Res.* 271, 118–137.
- Metelkin, D., Vernikovsky, V.A., Kazansky, A.Y., Wingate, M.T.D., 2010. Late Mesozoic tectonics of Central Asia based on paleomagnetic evidence. *Gondwana Res.* 18, 400–419.
- Metcalf, I., 2013. Gondwana dispersion and Asian accretion: tectonic and palaeogeographic evolution of eastern Tethys. *J. Asian Earth Sci.* 66, 1–33.
- Metcalf, I., 2011. Tectonic framework and Phanerozoic evolution of Sundaland. *Gondwana Res.* 19, 3–21.
- Metcalf, I., 1996. Gondwanaland dispersion, Asian accretion and evolution of eastern Tethys. *Aust. J. Earth Sci.* 43, 605–623.
- Morley, C.K., Woganan, N., Sankumarn, N., Hoon, T.B., Alief, A., Simmons, M., 2001. Late Oligocene–Recent stress evolution in rift basins of Northern and Central Thailand: implications for escape tectonics. *Tectonophysics* 334, 115–150.

- McQuarrie, N., Robinson, D., Long, S., Tobgay, T., Grujic, D., Gehrels, G., Ducea, M., 2008. Preliminary stratigraphic and structural architecture of Bhutan: implications for the along-strike architecture of the Himalayan system. *Earth Planet. Sci. Lett.* 272, 105–117.
- Myrow, P.M., Hughes, N.C., Goodge, J.W., Fanning, C.M., Williams, I.S., Peng, S.-C., Bhargava, O.N., Tangri, S.K., Parcha, S.K., Pogue, K.R., 2010. Extraordinary transport and mixing of sediment across Himalayan central Gondwanaland during the Cambrian–Ordovician. *Geol. Soc. Am. Bull.* 122, 1660–1670.
- Myrow, P.M., Hughes, N.C., Searle, M.P., Fanning, C.M., Peng, S.-C., Parcha, S.K., 2009. Stratigraphic correlation of Cambrian–Ordovician deposits along the Himalaya: implications for the age and nature of rocks in the Mt. Everest region. *Geol. Soc. Am. Bull.* 121, 323–332.
- Meert, J.G., Lieberman, B.S., 2008. The Neoproterozoic assembly of Gondwana and its relationship to the Ediacaran-Cambrian radiation. *Gondwana Res.* 14 (1), 5–21.
- Meert, J.G., 2003. A synopsis of events related to the assembly of eastern Gondwana. *Tectonophysics* 362 (1), 1–40.
- Phillips, L., Verdel, C., Allen, C., Esterle, J., 2018. Detrital zircon U-Pb geochronology of Permian strata in the Galilee Basin, Queensland, Australia, *Austr. J. Earth Sci.* 65(4) 465–481.
- Peng, T.P., Wang, Y.J., Fan, W.M., Liu, D.Y., Shi, Y.R., Miao, L.C., 2006. SHRIMP zircon U-Pb geochronology of Early Mesozoic felsic igneous rocks from the

- southern Lancangjiang and its tectonic implications. *Sci. China Ser. D Earth Sci.* 49, 1032–1042.
- Pullen, A., Kapp, P., Gehrels, G.E., Vervoort, J.D., Ding, L., 2008. Triassic continental subduction in central Tibet and Mediterranean-style closure of the Paleo-Tethys Ocean. *Geology* 36, 351–354.
- Poulsen, C.J., Pollard, D., Montañez, I.P., Rowley, D., 2007. Late Paleozoic tropical climate response to Gondwanan deglaciation. *Geology* 35, 771–774.
- Pourteau, A., Smit, M.A., Li, Z.-X., Collins, W.J., Nordsvan, A.R., Volante, S., Li, J., 2018. 1.6 Ga crustal thickening along the final Nuna suture. *Geology* 46, 959-962.
- Song, S.G., Niu, Y.L., Wei, C.J., Ji, J.Q., Su, L., 2010. Metamorphism, anatexis, zircon ages and tectonic evolution of the Gongshan block in the northern Indochina continent-an eastern extension of the Lhasa Block. *Lithos* 120 (3), 327–346.
- Song, S.G., Ji, J.Q., Wei, C.J., Su, L., Zheng, Y.D., Song, B., Zhang, L.F., 2007. Early Paleozoic granite in Nujiang River of northwest Yunnan in SW China and its tectonic implications. *Chinese Sci. Bull.* 52, 2402–2406 (in Chinese with English abstract).
- Sone, M., Metcalfe, I., 2008. Parallel Tethyan sutures in mainland Southeast Asia: new insights for Palaeo-Tethys closure and implications for the Indosinian orogeny. *Compt. Rendus Geosci.* 340 (2), 166–179.
- Tapponnier, P., Peltzer, G., Armijo, R., 1986. On the mechanics of the collision between India and Asia. In: Coward, M.P., Ries, A.C. (Eds.), *Collision Tectonics*. *Geol. Soc. Lond. Spec. Publ.* 19, 115–157.

- Torsvik, T.H., Cocks, L.R.M., 2009. The Lower Palaeozoic palaeogeographical evolution of the northeastern and eastern peri-Gondwanan margin from Turkey to New Zealand, in *Early Paleozoic Peri-Gondwana Terranes: new insights from tectonics and biogeography*, edited by Bassett, M. G. Geol. Soc. Spec. Publ. 325, 3–21.
- Ueno, K., 2003. The Permian fusulinoidean faunas of the Sibumasu and Baoshan blocks: their implications for the paleogeographic and paleoclimatologic reconstruction of the Cimmerian Continent. *Palaeogeogr. Palaeoclimatol. Palaeoecol.* 193, 1–24.
- van Hinsbergen, D.J.J., Kapp, P., Dupont-Nivet, G., Lippert, P.C., DeCelles, P.G., Torsvik, T.H., 2011. Restoration of Cenozoic deformation in Asia and the size of Greater India. *Tectonics* 30, TC5003.
- Veevers, J., Saeed, A., Belousova, E., Griffin, W., 2005. U-Pb ages and source composition by Hf-isotope and trace-element analysis of detrital zircons in Permian sandstone and modern sand from southwestern Australia and a review of the paleogeographical and denudational history of the Yilgarn Craton. *Earth Sci. Rev.* 68, 245–279.
- Veevers, J.J., 2004. Gondwanaland from 650–500 Ma assembly through 320 Ma mergers in Pangea to 185–100 Ma breakup: supercontinental tectonics via stratigraphy and radiometric dating. *Earth Sci. Rev.* 68, 1–132.
- Wiedenbeck, M., Allé, P., Corfu, F., Griffen, W.L., Meier, M., Oberli, F., von Quadt, A., Roddick, J.C., Spiegel, W., 1995. Three natural zircon standards for U-Th-Pb, Lu-Hf, trace element, and REE analyses. *Geostand. Geoanal. Res.* 19, 1–23.

- Wang, F., Liu, F.L., Schertl, H.P., Liu, P.H., Ji, L., Cai, J., Liu, L.S., 2019a. Paleotethyan tectonic evolution of Lancangjiang metamorphic complex: Evidence from SHRIMP U-Pb zircon dating and $^{40}\text{Ar}/^{39}\text{Ar}$ isotope geochronology of blueschists in Xiaoheijiang-Xiayun area, Southeastern Tibetan Plateau, Gondwana Res. 65, 142–155.
- Wang, H.N., Liu, F.L., Li, J., Sun, Z.B., Ji, L., Tian, Z.H., Liu, L.S., Santosh, M. 2019b. Petrology, geochemistry and P-T-t path of lawsonite-bearing retrograded eclogites in the Changning-Menglian orogenic belt, southeast Tibetan Plateau. J. Metamorph Geol. 37, 439–478.
- Wang, B., Wang, L., Chen, J., Yin, F., Wang, D., Zhang, W., Chen, L., Liu, H., 2014. Triassic three-stage collision in the Paleo-Tethys: Constraints from magmatism in the Jiangda-Deqen-Weixi continental margin arc, SW China. Gondwana Res. 26, 475–491.
- Wang, Y.J., Fan, W.M., Zhang, Y.H., Peng, T.P., Chen, X.Y., Xu, Y.G., 2006. Kinematics and $^{40}\text{Ar}/^{39}\text{Ar}$ geochronology of the Gaoligong and Chongshan shear systems, western Yunnan, China: implications for early Oligocene tectonic extrusion of SE Asia. Tectonophysics 418, 235–254.
- Wang, X.D., Ueno, K., Mizuno, Y., Sugiyama, T., 2001. Late Paleozoic faunal, climatic and geographic changes in the Baoshan block as a Gondwana-derived continental fragment in Southwest China. Palaeogeogr. Palaeoclimatol. Palaeoecol. 170, 197–218.
- Wang, Y.J., Qian, X., Cawood, P.A., Liu, H.C., Feng, Q.L., Zhao, G.C., Zhang, Y.H.,

- He, H.Y., Zhang, P.Z., 2018. Closure of the East Paleotethyan Ocean and amalgamation of the Eastern Cimmerian and Southeast Asia continental fragments. *Earth-Sci. Rev.* 186, 195–230.
- Xu, Y.C., Yang, Z.Y., Tang, Y.B., Wang, H., Gao, L., An, C.Z., 2015. Further paleomagnetic results for lower Permian basalts of the Baoshan Terrane, southwestern China, and paleogeographic implications. *J. Asia Earth Sci.* 104, 99–114.
- YNGMR (Yunnan Bureau of Geology and Mineral Resources), 1990. Regional Geology of Yunnan Province. Geological Publishing House, Beijing, pp. 45–201 (in Chinese with English abstract).
- Yin, A., 2010. Cenozoic tectonic evolution of Asia: a preliminary synthesis. *Tectonophysics* 488, 293–325.
- Yao, J.L., Shu, L.S., Santosh, M., 2011. Detrital zircon U-Pb geochronology, Hf isotopes and geochemistry - new clues for the Precambrian crustal evolution of Cathaysia block, South China. *Gondwana Res.* 20, 553–567.
- Zhao, T.Y., Feng, Q.L., Metcalfe, I., Milan, L.A., Liu, G.C., Zhang, Z.B., 2017. Detrital zircon U-Pb-Hf isotopes and provenance of Late Neoproterozoic and Early Paleozoic sediments of the Simao and Baoshan blocks, SW China: Implications for Proto-Tethys and Paleo-Tethys evolution and Gondwana reconstruction. *Gondwana Res.* 51, 193–208.
- Zhai, Q.G., Jahn, B.M., Wang, J., Hu, P.Y., Chung, S.L., Lee, H.Y., Tang, S.H., Tang, Y., 2016. Oldest Paleo-Tethyan ophiolitic mélange in the Tibetan Plateau. *GSA*

Bull. 128, 355–373.

Zhai, Q.G., Jahn, B.-m., Wang, J., et al., 2013. The carboniferous ophiolite in the middle of the Qiangtang terrane, northern Tibet: SHRIMP U–Pb dating, geochemical and Sr-Nd-Hf isotopic characteristics. *Lithos* 168-169, 186–199.

Zhai, Q.G., Zhang, R.Y., Jahn, B.M., Li, C., Song, S.G., Wang, J., 2011. Triassic eclogites from central Qiangtang, northern Tibet, China: petrology, geochronology and metamorphic P–T path. *Lithos* 125, 173–189.

Zhong, D., 1998. Paleo-Tethyan Orogenic Belt in Western Yunnan and Sichuan. Science Press, Beijing (in Chinese).

Zhu, D.C., Zhao, Z.D., Niu, Y., Dilek, Y., Mo, X.X., 2011. Lhasa terrane in southern Tibet came from Australia. *Geology* 39, 727–730.

Zhang, X.R., Chung, L.S., Lai, Y.M., Ghani, A., Murtadha, S., Lee, H.Y., Hsu, C.C., 2018. Detrital zircons dismember Sibumasu in East Gondwana. *J. Geophys. Res.* 123(7), 6068–6110.

Figure Captions

Fig.1. (A) Tectonic sketch of Southeast Asia (modified from Song et al., 2010). (B) Simplified geological map of the Gongshan-Baoshan area. (C) Stratigraphic columns from the Gongshan-Baoshan area. GB-Gongshan Block, TB=Tengchong Block, BB-Baoshan Block, LSB- Lanping-Simao Block, LSZ- Lanchangjiang suture zone. 1-Chongshan Fault, 2- Gaoligong Fault.

Fig.2. Field photographs and photomicrographs from the Late Paleozoic to Mesozoic strata in the Gongshan-Baoshan Block. (A) Triassic strata showing light gray siltstone interbedded with limestone. (B) Permian sandstone with centimeter- to meter-thick stratification. (C) Siltstone showing an foliated structure with fine-grained quartz and white mica. (D) Permian sandstone showing with a tectonic fabric in grains of quartz, mica and minor feldspar.

Fig.3. Representative CL images of detrital zircons from the Permian to Mesozoic strata in the Gongshan-Baoshan Block. U-Pb analysis spots are shown by red dotted circles.

Fig.4. LA-ICP-MS detrital zircon U-Pb concordia age plots and relative probability density diagrams of the Triassic strata in the Gongshan sub-terrane. n = Total number of detrital zircon analyses.

Fig.5. LA-ICP-MS detrital zircon U-Pb concordia age plots and relative probability density diagrams of the Permian strata in the Baoshan sub-terrane. n = Total number of detrital zircon

analyses.

Fig.6. LA-ICP-MS detrital zircon U-Pb concordia age plots and relative probability density diagrams of the Jurassic strata in the Baoshan sub-terrane. n = Total number of detrital zircon analyses.

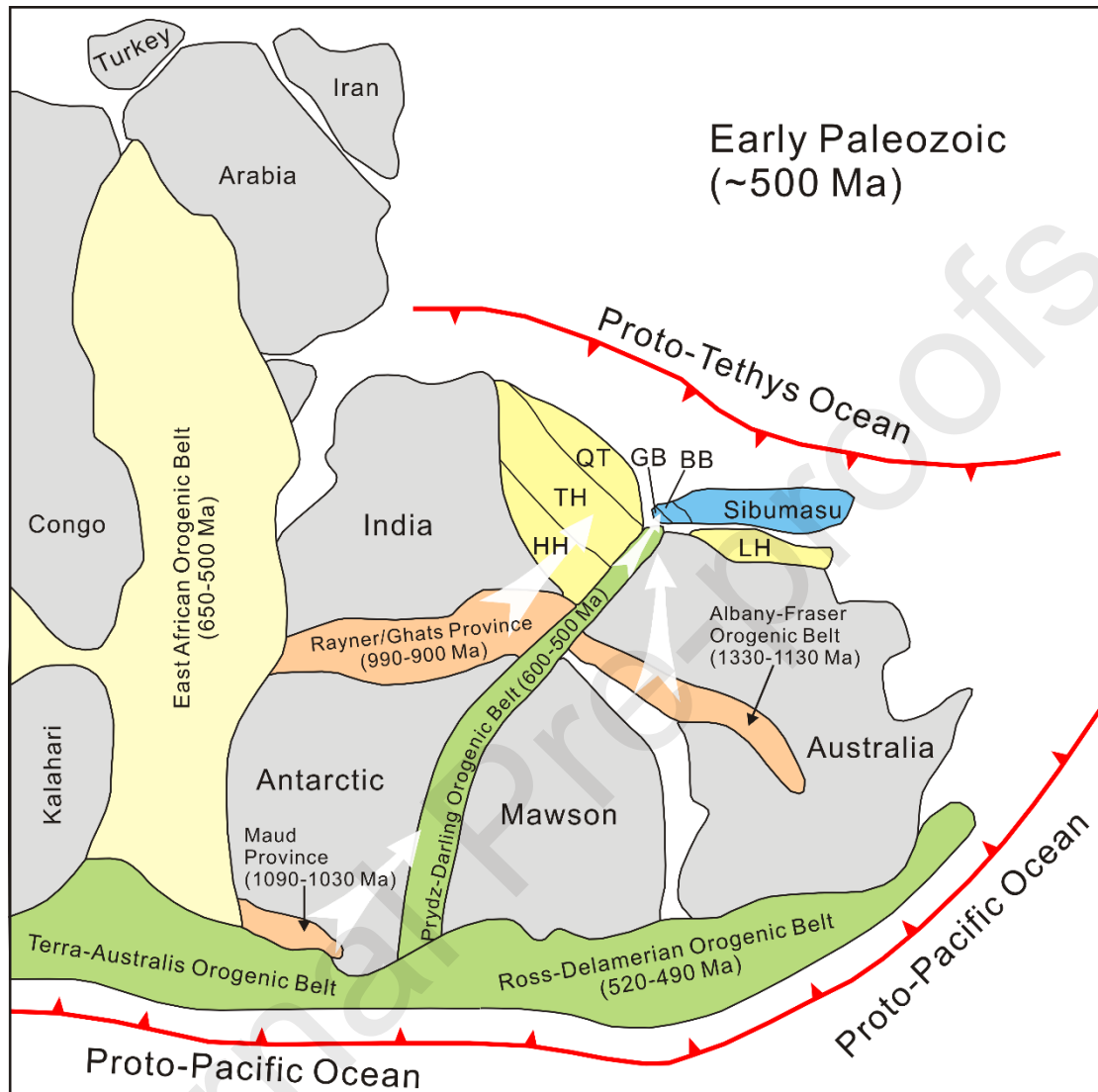
Fig.7. Comparison of the relative probability density diagrams of detrital zircon ages between the Gongshan-Baoshan Block and East Gondwana-derived blocks. Data sources are: Sibumasu Terrane, Cai et al. (2017); Western Australia, Cawood and Nemchin (2000) and Veevers et al. (2005); Eastern Australia, Phillips et al. (2018); Lhasa Block, Leier et al. (2007) and Zhu et al. (2011); Western Qiangtang, Pullen et al. (2008), Dong et al. (2011) and Zhu et al. (2011); Tethyan Himalaya, McQuarrie et al. (2008), Myrow et al. (2009, 2010) and Zhu et al. (2011); Cathaysia Block, Yao et al. (2011), High Himalaya, Gehrels et al. (2006a, 2006b). N = Total number of samples; n = Total number of detrital zircon analyses.

Fig.8. A tentative reconstruction of the Gongshan-Baoshan Block in East Gondwana during the Early Paleozoic (~500 Ma), modified from Metcalfe (2013) and Ali et al. (2013). GB-Gongshan Block, BB-Baoshan Block, LH-Lhasa Block, QT-Qiangtang, TH-Tethyan Himalaya, HH-High Himalaya. The white arrows are hypothetical sediment pathways.

Highlights

- Detrital zircons of the Gongshan-Baoshan Block reveal a secular episodic continental growth of Gondwana.
- The Gongshan-Baoshan Block was located along the northwestern margin of Australia before segmentation of Gondwana.
- The subduction of the Paleo-Tethys Ocean initiated at ~273 Ma and ended at ~223 Ma.

Graphical abstract



Declaration of interests

The authors declare that they have no known competing financial interests or personal relationships that could have appeared to influence the work reported in this paper.

The authors declare the following financial interests/personal relationships which may be considered as potential competing interests:

Yingtian Song
Li Su
Jinlong Dong
Shuguang Song
Mark B. Allen
Chao Wang
Xiaolan Hu

Journal Pre-proofs